ity to the transcription machinery or its direct interaction with general transcription factors. As a consequence, increased amounts of HNF-1 induce a regulatory mechanism that leads to the general down-regulation of HNF-4–dependent liver-specific genes, including the HNF-1 gene itself. This promoter-dependent dual function of HNF-1 suggests its central role in the coordination of the regulatory network that defines the hepatic phenotype.

REFERENCES AND NOTES

1. M. Frain *et al.*, *Cell* **59**, 145 (1989); S. Baumhueter *et al.*, *Genes Dev.* **4**, 372 (1990); V. De Simone *et al.*, *EMBO J.* **10**, 1435 (1991); W. H. Landschulz, P. F. Johnson, E. Y. Adashi, B. J. Graves, S. L. McKnight, *Genes Dev.* **2**, 786 (1988); E. Lai *et al.*, *ibid.* **4**, 1427 (1990); F. M. Sladek, W. Zhong, E. Lai, J. E. Darnell Jr., *ibid.*, p. 2353.
2. C. J. Kuo *et al.*, *Nature* **355**, 457 (1992); H.-M. Tian and U. Schibler, *Genes Dev.* **5**, 2225 (1991).
3. A. A. Kritis, E. Ktistaki, D. Barda, V. I. Zannis, I. Talianidis, *Nucleic Acids Res.* **21**, 5882 (1993).
4. G. Piaggio *et al.*, *ibid.* **22**, 4284 (1994).
5. M. Mietus-Snyder *et al.*, *Mol. Cell. Biol.* **12**, 1708 (1992); J. A. A. Ladias *et al.*, *J. Biol. Chem.* **267**, 15849 (1992); I. Talianidis, A. Tambakaki, J. Toursounova, V. I. Zannis, *Biochemistry* **34**, 10298 (1995).
6. F. Tronche *et al.*, in *Liver Gene Expression*, F. Tronche and M. Yaniv, Eds. (Landes, Austin, TX, 1994), chap. 9.
7. W. Zhong, J. Mirkovitch, J. E. Darnell Jr., *Mol. Cell. Biol.* **14**, 7276 (1994).
8. M. Pontoglio *et al.*, Cell **84**, 575 (1996).
9. D. B. Mendel *et al.*, *Science* **254**, 1762 (1991).
10. E. Ktistaki and I. Talianidis, unpublished data.
11. M. F. Carey, H. Kakidani, J. Leatherwood, F. Mostashari, M. Ptashne, *J. Mol. Biol.* **209**, 423 (1989).
12. F. M. Sladek, in (*6*), chap. 11.
13. E. Ktistaki, J. M. Lacorte, N. Katrakili, V. I. Zannis, I. Talianidis, *Nucleic Acids Res.* **22**, 4689 (1994); E. Ktistaki, N. T. Ktistakis, E. Papadogeorgaki, I. Talianidis, *Proc. Natl. Acad. Sci. U.S.A.* **92**, 9876 (1995); A. A. Kritis *et al.*, *Gene* **173**, 275 (1996).
14. E. Ktistaki and I. Talianidis, *Mol. Cell. Biol.* **17**, 2790 (1997).
15. D. B. Smith and K. S. Johnson, *Gene* **67**, 31 (1988).

16. We thank A. Economou for critical reading of the manuscript. Supported by Greek General Secretary for Science and Technology grant PENED2018.

7 February 1997; accepted 13 May 1997

Positive Effects of Combined Antiretroviral Therapy on CD4$^+$ T Cell Homeostasis and Function in Advanced HIV Disease

B. Autran,* G. Carcelain, T. S. Li,† C. Blanc,† D. Mathez, R. Tubiana, C. Katlama, P. Debré, J. Leibowitch

Highly active antiretroviral therapy (HAART) increases CD4$^+$ cell numbers, but its ability to correct the human immunodeficiency virus (HIV)–induced immune deficiency remains unknown. A three-phase T cell reconstitution was demonstrated after HAART, with: (i) an early rise of memory CD4$^+$ cells, (ii) a reduction in T cell activation correlated to the decreasing retroviral activity together with an improved CD4$^+$ T cell reactivity to recall antigens, and (iii) a late rise of "naïve" CD4$^+$ lymphocytes while CD8$^+$ T cells declined, however, without complete normalization of these parameters. Thus, decreasing the HIV load can reverse HIV-driven activation and CD4$^+$ T cell defects in advanced HIV-infected patients.

New antiretroviral therapies combining inhibitors of HIV-1 protease and reverse transcriptase are highly efficient at reducing viral replication and increasing CD4$^+$ T cell numbers (*1*). The physiopathological processes that allow such CD4$^+$ T cell increases are debated as is the capacity of such treatments to allow CD4$^+$ cell regeneration and restoration of immune competence. These sets of questions reflect current controversies about the pathogenesis of HIV-related CD4$^+$ cell depletion. Indeed, although much attention has been paid to the high turnover in HIV virions and infectious CD4$^+$ T cells (*2*), no evidence for an enhanced turnover and regeneration in the mature CD4$^+$ subset has been produced so far, either in the course of the natural HIV infection or after HAART (*3*). Telomer length studies have indeed provided evidence for a high turnover in the CD8$^+$ but not in the CD4$^+$ subset (*4*). Furthermore, reduced numbers of phenotypically defined "naïve" T cells in advanced HIV-infected patients argue for a decline in the T cell regeneration capacity with disease progression, although mechanisms for such defects are not elucidated (*5*). On the other hand, the chronic T cell activation observed throughout the course of infection favors T cell apoptosis or anergy, or both, which might contribute to the CD4$^+$ T cell depletion, though also affecting the undepleted CD8$^+$ cell subset (*6*). A progressive CD4$^+$ cell dysfunction also appears on a per-cell basis in early stages of the disease, as assessed in vitro by defects in CD4$^+$ T cell proliferation and interleukin-2 (IL-2) production to recall antigens (*7*), and might participate in the loss of mature T cell expansion with disease progression.

We investigated the extent to which HAART would reverse these major CD4$^+$ T cell abnormalities and allow some restoration of immune competence at advanced stages of HIV disease. We analyzed expression of key surface molecules on peripheral blood T cells and the CD4$^+$ T cell proliferation against recall antigens from two major opportunistic infections under potent antiretroviral regimens. Eight previously untreated adults with advanced HIV-1 infection received ritonavir, a potent HIV-1 protease inhibitor, combined with azidothymidine (AZT) and dideoxycytosine, two reverse transcriptase inhibitors, over a period of 12 months. Ritonavir given alone the first 2 weeks rapidly induced a 1.3 ± 0.5 log decrease ($P = 0.01$) in the numbers of both HIV RNA copies per milliliter of plasma and infectious cells per 10^7 blood mononuclear cells from base-line values of 4.9 ± 0.4 and 3.4 ± 0.5, respectively ($P < 0.05$). A maximal decline of 1.9 ± 0.6 log and 2.5 ± 0.5 log was reached for each viral parameter at month 6 under triple-combination therapy (Fig. 1). A low stable viral load was maintained under treatment through month 12 with plasma HIV-1 RNA copies falling below the threshold of detection in three of the eight patients. Major T cell changes were also observed in the peripheral blood from all patients during the first 2 weeks of treatment. A steep rise occurred in lymphocyte counts that predominated on the CD4$^+$ subset, with a twofold CD4$^+$ cell increase from a mean base line of 164 ± 86 cells/μl of plasma to 327 ± 74 cells/μl of plasma ($P = 0.01$). Meanwhile, CD8$^+$ cells also increased, though with a lower amplitude from a mean of 1168 ± 427 cells/μl plasma at entry to 1387 ± 619 cells/μl plasma at day 15 ($P = 0.035$). During the next 12 months, a sustained though slower CD4$^+$ cell increase was observed with a mean positive linear slope of +10%. The CD4$^+$ cells reached a mean value of 365 ± 145 cells/μl plasma 1 year after initiation of the study, however, remaining below normal ranges in six of the eight patients (mean normal CD4 counts were 900 ± 185 cells/μl plasma). In contrast, CD8$^+$ cells, as

B. Autran, G. Carcelain, T. S. Li, C. Blanc, P. Debré, Laboratoire d'Immunologie Cellulaire, URA CNRS 625, Hôpital Pitié-Salpétrière, 47-83 Boulevard de l'Hôpital, Paris, France.
D. Mathez and J. Leibowitch, Service d'Immunologie Hématologie, Hôpital Raymond Poincaré, Garches, France.
R. Tubiana and C. Katlama, Service de Maladies Infectieuses et Tropicales, Hôpital Pitié-Salpétrière, Paris, France.

*To whom correspondence should be addressed. E-mail: autran@psl.ap-hop-paris.fr
†These authors contributed equally to this work.

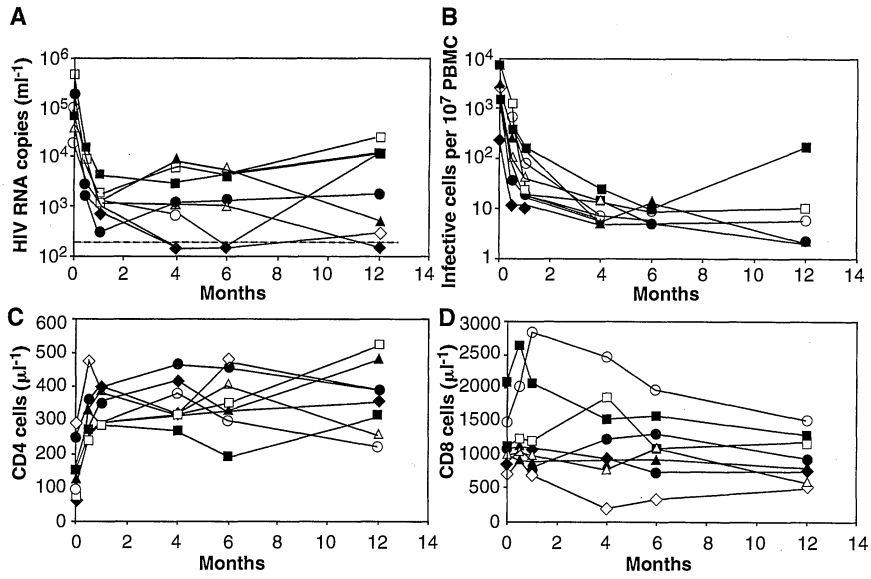

Fig. 1. Long-term changes in CD4 and CD8 lymphocyte counts, plasma viral load, and cellular viremia under triple antiretroviral therapy. Eight non–drug experienced patients (mean age, 38; age range of 32 to 50) were enrolled in a multicenter open study approved by the ethical review boards. Participants had no prior antiretroviral therapy and gave written informed consent before entering the study. Patients received 600 mg/day of ritonavir (Abbott Laboratories) for 14 days, after which were added 600 mg/day of zidovudine (Retrovir, Glaxo-Wellcome) and 6 mg/day of zalcitabine (Hivid, Roche) with treatment maintenance for 12 months. (**A**) Plasma HIV RNA copies/ml were determined by reverse transcriptase polymerase chain reaction (PCR) (Roche Molecular Systems, Amplicor kit). The threshold detection level was 200 HIV RNA copies/ml (dashed line). Results are expressed as the numbers of HIV-1 RNA copies (log 10) per milliliter of plasma; (**B**) Number of infectious cells was determined by co-culture of patient peripheral blood mononucleated cells (PBMCs) isolated on Ficoll-Paque gradient centrifugation with allogeneic phytohemagglutinin-blasts and IL-2 and analyzed according to Poisson distribution analysis (*23*). (**C**) Blood CD4$^+$ and CD8$^+$ T lymphocyte percentages were analyzed according to standard procedures from fresh EDTA-blood samples with a flow cytometer (Becton Dickinson, San Jose, California); absolute cells per microliter were derived from total blood lymphocyte counts obtained from automated totalleukocyte counts (Coulter, Margency, France). (**D**) Blood CD8$^+$ counts were determined as described above. Normal values for CD4 cells are 900 ± 185 cells/µl plasma and for CD8 cells are 550 ± 165 cells/µl plasma. Intrapatient variations were calculated by using the Wilcoxon ranked nonparametric test.

well as total lymphocyte counts (*8*), declined in the same period to a mean of 966 ± 480 cells/µl plasma, still above normal values (550 ± 165 cells/µl plasma) in six of eight patients. The T cell differentiation and activation changes were further assessed on cryopreserved cells. The initial increase in lymphocyte counts was due to CD3$^+$ T cell changes as their numbers increased from 59 ± 12% to 77 ± 11% at 4 months ($P = 0.012$), whereas B and natural killer lymphocyte percentages decreased (*8*). The percentages of CD3$^+$CD4$^+$ T cells continuously increased from 12 ± 9% at entry to 18 ± 6% 12 months later ($P = 0.028$). However, they remained far below normal values (45 ± 7%) (*8*), thus reflecting the persistent predominance of the CD8$^+$ lymphocyte subset.

Memory CD4$^+$ T cells, as defined by the CD45RO isoform usage (*9*), primarily contributed to this CD4$^+$ T cell increase ($P < 0.05$) during the first 4 months of the study. A second though nonsignificant rise occurred between months 6 and 12, where they accounted for a mean of 75 ± 5% of the CD4$^+$ T cell subset (normal is 55 ± 9%) (Fig. 2). Reciprocal findings were noted in the CD4$^+$45RA$^+$/RO$^-$ subset. Functional naïve CD4$^+$ T cells are better characterized by double expression of the CD45RA isoform plus the L-selectin (CD62L), as the latter facilitates the cells' entry in the lymph nodes through the high endothelial venules (*10, 11*). More important, in these untreated advanced patients,

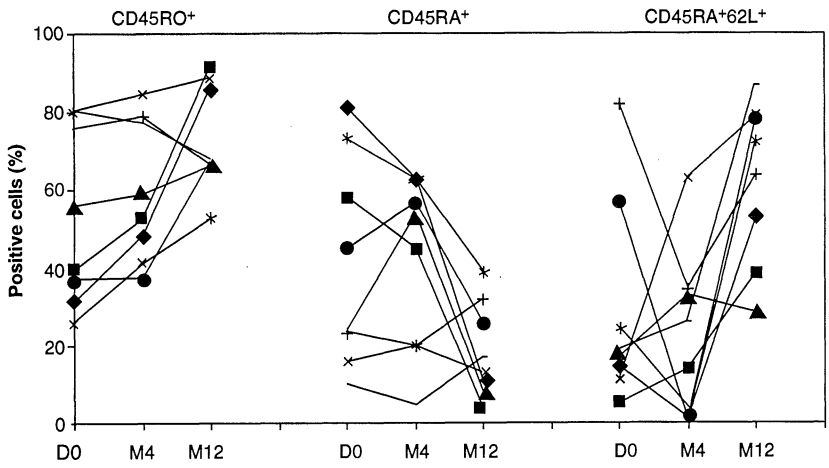

Fig. 2. Two-phase kinetics in memory/naïve CD4 T cell amplification. Patient PBMCs were separated on Ficoll-Hypaque gradient and kept frozen in liquid nitrogen until use under conditions yielding ≥80% cell viability upon thawing. The proportions of CD4 memory (CD45RO$^+$) or naïve (CD45RA$^+$ and CD45RA$^+$CD62L$^+$) subsets were assessed on thawed PBMCs by three- and four-color immunofluorescence (IF) analysis using the following monoclonal antibodies (mAbs): anti-CD4 (SFCI12T4D11) mAb conjugated to energic couple dye (ECD), a tandem fluorochrom composed of phycoerythrin (PE) and Texas Red; fluorescein isothiocyanate (FITC)–conjugated mAbs against: CD3 (IOT3b), CD45RA (ALB11), CD45RO (UCHL-1), and CD62L (DREG58). Isotype-matched control murine immunoglobulins were conjugated to the distinct fluorochroms defined above. All reagents were a gift from Coultronics (Margency, France). Cells were simultaneously stained with distinct fluorescent-labeled mAbs in phosphate-buffered saline supplemented with 1% bovine serum albumin, washed, and analyzed (10,000 cells per sample) on an EPICS XL II cytometer with the tetraOne™ software (Coulter). Percentages of CD4$^+$ and CD3$^+$CD4$^+$ cells were found to be identical; therefore, the following analysis was performed on CD4$^+$ cells: CD4$^+$ CD45RO$^+$ and CD45RA$^+$ cell percentages in the CD4$^+$ subset were determined in a lymphocyte gate defined on forward and side scatters (FSC/SSC) [that contained a total of CD3$^+$, CD19$^+$, and CD16$^+$CD56$^+$ lymphocytes >95%, as defined on separate samples (*8*)] combined to a CD4$^+$ gate. The CD62L positivity was analyzed on the CD4$^+$CD45RA$^+$ cells by successively combining the FSC/SSC, CD4$^+$, and CD45RA$^+$ gates. Normal values are as follows: CD3$^+$4$^+$ and CD4$^+$ T cells, 900 ± 185 cells/µl plasma; CD4$^+$CD45RO$^+$ in CD4$^+$ cells, 55 ± 9%; CD4$^+$CD45RA$^+$ in CD4$^+$ cells, 47 ± 10%; and CD62L$^+$ in CD4$^+$ CD45RA$^+$ cells, 96 ± 3%. All samples corresponding to the same patient were analyzed in the same experiment. Results are presented as individual percentages of positive cells at day 0 (D0), month 4 (M4), and 12 (M12) after treatment. Intrapatient variations were calculated with the Wilcoxon ranked nonparametric test.

the proportions of L-selectin$^+$ cells were extremely low before treatment, representing a mean of 23 ± 25% in the CD4$^+$ CD45RA$^+$ subset compared with their normal (96 ± 3%) values. These low CD62L$^+$ percentages were maintained for 4 months after initiation of therapy. Around that time, the proportions of L-selectin$^+$ cells steadily increased within the CD4$^+$ CD45RA$^+$ subset to reach a mean 62 ± 25% ($P < 0.05$) (Fig. 2), still lower than the control values observed in healthy HIV-1 seronegative adults. The overall changes resulted in a twofold increase in absolute values of naïve L-selectin$^+$CD4$^+$ T cells from the base line.

The two waves in memory and naïve CD4$^+$ T cells were associated with a decrease in CD4$^+$ T cell activation markers. Indeed, a continuous decrease in the proportions of activated CD4$^+$ T cells displaying major histocompatibility complex class II molecules [human lymphocyte antigen–DR (HLA-DR)] was noted from day 15 to month 12 ($P = 0.011$) when they reached normal values (Fig. 3A). The loss in HLA-DR expression predominated on memory CD4$^+$45RO$^+$ T cells, a point of special importance when the preferential propagation of HIV in activated cells from this subset is considered (*12*). A transient early rise in CD4$^+$ T cells displaying the α chain of the IL-2 receptor (CD25) was noted at day 15 mostly on memory CD4$^+$45RO$^+$ T cells, followed by a reduction in CD4$^+$CD25$^+$ cells at month 4 to normal values ($P = 0.025$) (Fig. 3B). Eventually, a significant increase of CD25$^+$ cells occurred in the CD4$^+$CD45RA$^+$ subset ($P = 0.028$) during the last 6 months in parallel to the late increase of the CD4$^+$45RA$^+$62L$^+$ cells. Contrasting with the early IL-2–R-α chain changes, the CD69, a very early marker of lymphocyte activation and proliferation (*13*), was barely detected (<1%) on CD4$^+$ T cells even during the early lymphocyte rise. Similarly, no propidium iodide nuclear incorporation (a marker for cycling cells) was detected in these peripheral blood CD4$^+$ T cells (8). Activation markers also declined in the CD8$^+$ subset during the study period, and the proportions of activated CD8$^+$CD3$^+$ T cells displaying HLA-DR reached normal values at month 12 ($P = 0.043$) (Fig. 3A). The kinetics in CD3$^+$8$^+$HLA-DR$^+$ cell decrease was similar to the decrease in CD3$^+$4$^+$HLA-DR$^+$ cells and occurred in parallel with the progressive decline in CD8$^+$ counts. High proportions of CD8$^+$ T cells exhibiting CD38 indicated the advanced disease stage of our patients before treatment (*14*). The CD38 expression also decreased on CD8$^+$CD38$^+$ cells over the study period, from 75 ± 17% of cells strongly CD38$^+$ at day 0 to a mean of 55 ± 23% of cells weakly CD38$^+$ at month 12 ($P = 0.011$), which was close to normal values (41 ± 18%). A strong decrease in CD38 fluorescence intensity was observed between day 0 and month 6 (Fig. 4). Interestingly, a strong correlation ($r^2 > 0.8$) was found over the 12-month study period between the decreasing HIV activity and the subsiding activation markers HLA-DR and CD38 on both CD4$^+$ and CD8$^+$ T cells. The HIV-related abnormalities in T cell activation and differentiation therefore were, in part, reversible with viral load reduction in advanced patients.

We then investigated whether a defective CD4$^+$ T cell proliferation to recall antigens might be corrected under treatment in a second independent study. Six non-pretreated patients with similar viral load and CD4 counts received a similar combined regimen. A reduction of 3 log in plasma viral load was observed 3 months after therapy together with a mean absolute

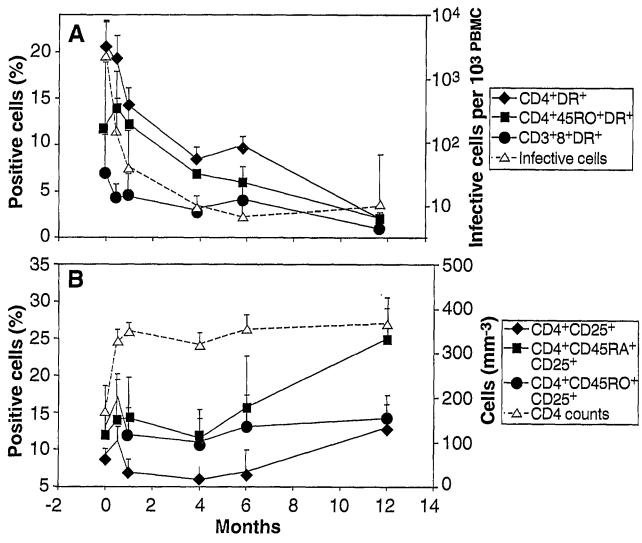

Fig. 3. Decreased T cell activation and viral load under triple antiretroviral therapy. Changes in T cell activation markers HLA-DR and CD25 were measured on CD4$^+$ and CD8$^+$ T cell subsets by three-color IF analysis of frozen cells. (**A**) Changes in HLA-DR expression on CD4$^+$, CD4$^+$ CD45RO$^+$, and CD3$^+$CD8$^+$ T cells. Procedures described in Fig. 2 were used: CD8$^+$ T cells were labeled with a FITC-conjugated anti-CD3 (IOT3b) and an ECD-conjugated anti-CD8 (CFCI21Thy203) mAbs; HLA-DR was labeled by using the PE–cyanine 5 (PE-Cy5)–conjugated anti-HLA-DR mAb (Immu 257), (Coulter). The HLA-DR positivity was analyzed on the previously defined CD4$^+$, and CD4$^+$CD45RO$^+$ cells by successively combining the FSC/SSC, the CD4$^+$, and the CD45RO$^+$ gates, and on CD8$^+$ T cells by successively combining the FSC/SSC, CD3$^+$, and CD8$^+$ gates. Normal values for HLA-DR$^+$ positivity in the CD4$^+$ and CD8$^+$ subsets were 6 ± 3% and 10 ± 6%, respectively. Results are expressed as mean ± SE percentages of HLA-DR$^+$ cells within either the CD4$^+$, the CD4$^+$CD45RO$^+$, or the CD3$^+$CD8$^+$ cells. Cellular viremia is also shown as defined in Fig. 1. Results are expressed as the mean ± SD values. Intrapatient variations were calculated with the Wilcoxon ranked nonparametric test. (**B**) Changes in CD25 expression in the CD4$^+$, CD4$^+$CD45RO$^+$, and CD4$^+$CD45RA$^+$ cells were defined according to the procedures described in Fig. 2 and using a PE-conjugated anti-CD25 (B1-49-9) mAb clone (Coulter). Percentages of CD4$^+$CD25$^+$ cells in the CD4$^+$ cells were determined in a FSC/SSC lymphocyte gate combined to a CD4$^+$ gate. The CD25 positivity was analyzed on the previously defined CD4$^+$CD45RO$^+$ and CD4$^+$CD45RA$^+$ cells by successively combining the FSC/SSC, CD4$^+$, and CD45RO$^+$ or CD45RA$^+$ gates. Results are expressed as mean ± SE percentages of positive cells within either the CD4$^+$, the CD4$^+$CD45RO$^+$, or the CD4$^+$CD45RA$^+$ cells. Normal values for CD4$^+$CD25$^+$ in the CD4$^+$ subset are 6 ± 7%. Mean absolute CD4 counts measured on fresh blood samples as defined in Fig. 1 are also shown.

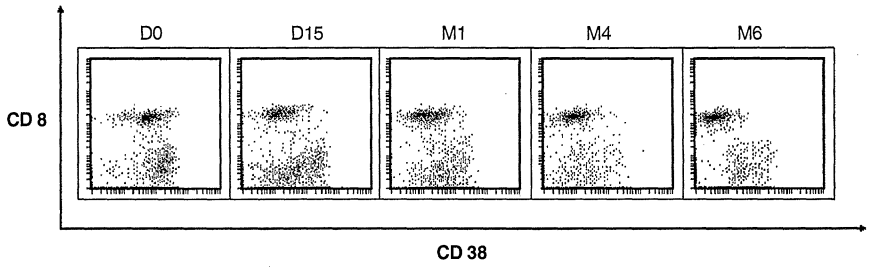

Fig. 4. Decreased expression of CD38 on CD8$^+$ T cells under triple antiretroviral therapy. Changes in CD38 expression defined by three-color IF analysis of frozen cells, using the procedures described in Fig. 2 and the PE-conjugated CD38 (T16) mAb (Coulter). Expression of CD38 on CD8$^+$CD3$^+$ cells was analyzed by successive gating as described in Fig. 3. Normal values for percentages of CD8$^+$ cells positive for 41 ± 18 with a weak positivity of the CD38 expression. IF dot plot analysis of CD38 expression on CD8$^+$ T cells is given from a representative patient. All frozen samples were analyzed in a single experiment.

$CD4^+$ cell increase of 129 ± 95 cells/μl plasma above the base-line values of 176 ± 106 cells/μl plasma (Fig. 5A). Plasma HIV-1 RNA copies became undetected in three of six patients. Changes in naïve and memory $CD4^+$ T cells were similar to the changes reported above and further confirmed the late absolute increase in $CD4^+45RA^+62L^+$ naïve cells ($P = 0.02$) that, however, remained below normal thresholds (425 ± 150 cells/μl plasma) (Fig. 5A). In the six patients, we could not detect a significant in vitro proliferative response to recall antigens from cytomegalovirus (CMV) and *Mycobacterium tuberculosis* before treatment, which contrasts with the strong T cell proliferation induced by CD3-triggering (Fig. 5, B through D). A $CD4^+$ T cell proliferation against CMV and tuberculin antigens was detected after initiation of therapy while remaining negative against the HIV-1 p24 antigen (*8*). A significant increase in stimulation indexes against CMV and tuberculin occurred between month 1 and 6 in the six patients ($P < 0.05$) (Fig. 5, C and D). In addition, both the amplitude and the kinetics of such antigen-specific proliferative responses differed from the anti-CD3 mitogenic effect. Indeed, a maximal 13-fold increase in stimulation indexes from the base line was reached at month 3 for antigen-specific proliferation, which contrasted with the sixfold maximal increase observed for CD3-stimulation between day 15 and month 1. Such improved antigen-specific T cell reactivity was also detected on a per-cell basis as assessed by the significant increase in proliferation against CMV or tuberculin when analyzed per $CD4^+$ T cells from a mean of 55 ± 85 at entry up to 205 ± 120 cpm per 1000 $CD4^+$ T cells at month 6 ($P < 0.05$) (*8*). This antigen-specific proliferation reached normal ranges (mean normal indexes: 50 ± 40) for three of the six patients between months 3 and 6 (Fig. 5, C and D).

In these two studies, immune reconstitution was first marked by a rapid outburst in the circulation of both $CD8^+$ and mature memory $CD4^+$ T cells devoid of early markers of ongoing cell proliferation except for the transient peak in memory $CD4^+$ T cells displaying the α-chain receptor. Such features suggest that $CD4^+$ and $CD8^+$ T cells, previously recruited into productively infected tissues before treatment, would be mobilized and recirculate with the arrest in viral replication, as shown in murine models (*15*). Activation markers then subsided on both $CD4^+$ and $CD8^+$ T cells as retroviral activity decreased under antiretroviral drug control. Although we cannot exclude some non-antiviral effects of protease inhibitors (*16*), the lower HIV activity obtained with efficient antiviral therapy should result in a rapid subtraction of virus antigens in germinal centers, as recently shown (*17*), with opposite effects on the $CD4^+$ and $CD8^+$ T cell numbers. Lower HIV activity and the subsequent reversal of chronic T cell activation would thus allow for a slow $CD4^+$ T cell expansion, whereas the $CD8^+$ T cell compartment would contract. Memory $CD4^+$ T cells predominated in the early $CD4^+$ blood cell increase, while L-selectin$^+$ naïve $CD4^+$ T cells appeared later on, data reminiscent of the T

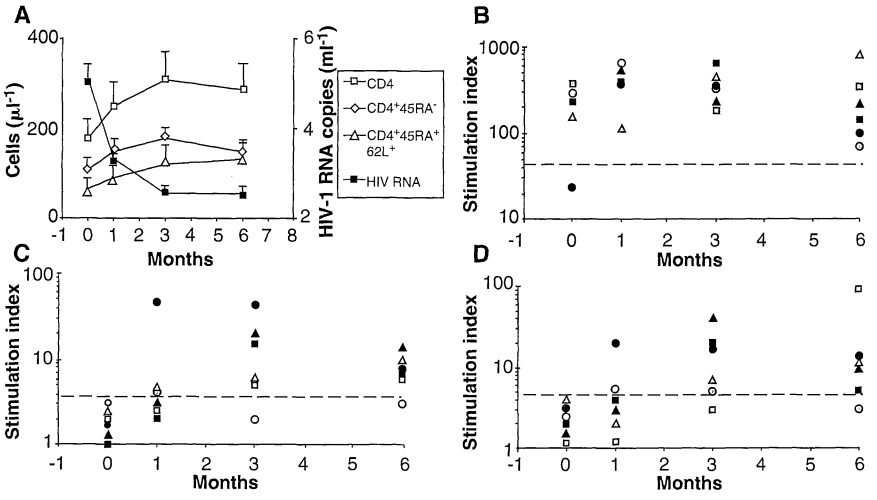

Fig. 5. Restoration of specific $CD4^+$ T cell reactivity to recall antigens under combined antiretroviral therapy. Six naïve patients with mean initial CD4 counts of 176 ± 106 cells/μl plasma and viral load of 5.3 ± 0.3 log HIV-1 RNA copies/ml received a combined antiretroviral regimen including one protease inhibitor (indinavir: Crixivan) plus two nucleoside analogs (AZT or D4T + 3TC) and were prospectively followed up for 6 months after initiation of therapy for CD4 T cell reconstitution. (**A**) Kinetics in the viral load decrease and absolute values in CD4 subsets reconstitution. Plasma viral RNA load was detected by reverse transcriptase PCR (Roche Amplicor Monitor kit). The threshold level of detection was 200 HIV RNA copies/ml. For each assay, a negative control, a low-level positive control (1000 to 3500 copies/ml), and a high-level positive control (500,000 to 700,000 copies/ml) were used. Flow cytometry analysis: the percentages and absolute counts of CD4, CD8 lymphocytes were detected from fresh samples with a four-color flow cytometer (Coultronics). The flow cytometry analysis of various CD4 subpopulations was performed on the same whole blood specimen in three-color IF, using a panel of mAbs to the following cell-surface proteins: CD3-PercP, CD4-FITC, CD8-PE, CD45-FITC/CD14-PE (Becton Dickinson, Pont de Clay, France) and CD45RA-PE, and CD62L-FITC (Immunotech, Marseille-Luminy, France). All antibodies were incubated with 100 μl of whole blood for 20 min at 20°C before red cell lysis. After washings with PBS, 5000 lymphocytes defined by an FSC/SSC gate combined to $CD45^+/CD14^-$ staining were acquired into the FACScan flow cytometer and analyzed according to Cell Quest (Becton Dickinson, San Jose, California). (**B**) T cell proliferation triggered by CD3 cross-linking: Proliferation assays were performed on fresh PBMC at the different time-points into microtiter plates previously coated by an anti-CD3 mAb (UCHT1, a gift of P. Beverley, IRCF, London, United Kingdom) from ascitic fluids at appropriate dilutions according to standard procedures (*24*). A total of 1×10^5 PBMCs containing a known percentage of $CD4^+$ T cells was cultured for 3 days in RPMI-1640 culture medium supplemented with 2 mM L-glutamine, 1 mM sodium pyruvate (Gibco Life Technologies, Cercy Pontoise, France), and 10% pooled heat-inactivated normal CMV-seronegative human AB sera (Centre de Transfusion Sanguine, Hôpital Pitié-Salpétrière, Paris, France). Tritiated thymidine (1 μCi) (CEA, Saclay, France) was added during the last 18 hours of culture and incorporated radioactivity was measured on a β scintillation counter (Beckman). Results were considered as positive only when meeting two conditions: geometric mean counts per minute with antigens >5000 and stimulation indexes (counts per minute obtained for cells+stimuli/cells+medium) >5. The threshold for normal values was ≥35,000 and index ≥35 cpm is indicated (dashed line). Antigen-specific $CD4^+$ T cell proliferation against CMV (**C**) and tuberculin (**D**) antigens. Proliferation assays were performed as described above against purified protein antigens from CMV (Behring, Germany) or tuberculin (Serum-Staat-Institut, Copenhagen, Denmark) that were extensively dialyzed and titrated before use at appropriate dilutions. Cells were cultured for 6 days. Similar assays were performed with the recombinant HIV-1 p24 protein produced in *Escherichia coli*, purified and extensively dialyzed (Transgène, Strasbourg, France). Positive antigen-specific responses were to meet two conditions: cpm >2000 and a stimulation index (SI) >3. The SI of 3 is indicated (dashed line). The mean SI normal values are 50 ± 40. Similar indexes were obtained when testing CD8-depleted cell preparations in similar conditions (*8*). The counts per minute results were also analyzed in relationship to the $CD4^+$ T cell input in culture by calculating the experimental counts per minute (CMV or tuberculin) per 1000 $CD4^+$ T cells in culture minus the control counts per minute without antigen per 1000 $CD4^+$ T cells (*8*). Intrapatient variations were calculated with the Wilcoxon ranked nonparametric test.

cell regeneration observed in adult recovery from bone-marrow aplasia that is mainly composed of memory $CD4^+$ T cells (*18*). The trend toward normalization of $CD4^+$ T cells displaying the CD28 costimulatory molecule (*8*) observed in our studies reflects the lower $CD4^+$ T cell activation and might allow for some recovery from enhanced sensitivity to apoptosis or anergy (*19*). The loss of memory $CD4^+$ T cell reactivity to recall antigens was indeed reversible under efficient antiviral therapy. This latter observation contrasts with the limited benefit for $CD4^+$ T cell function reported with ritonavir alone, where a weaker reduction in viral load (–1 log) could only increase preexisting $CD4^+$ T cell responses but failed to restore a lost T cell reactivity to recall antigens (*20*). The significant but partial restoration of $CD4^+$ T cell proliferation to recall antigens that we report might participate to the progressive regeneration of mature peripheral $CD4^+$ T cells observed after the first month of treatment, in agreement with murine models (*21*, *22*).

This sequence of events suggests that, in the natural course of a productive infection, HIV activity per se is the driving force for chronic immune stimulation; the latter would take part in the defects in antigen-specific $CD4^+$ T cell activation and proliferation noted in HIV-infected patients (*6*, *7*). Because such functions are required for a normal homeostasis of mature peripheral T cells in adults (*21*), their alteration would appear as a key mechanism in HIV-induced $CD4^+$ T cell depletion. This impairment of the mature $CD4^+$ cell repopulation process was, in part, reversible under effective antiviral treatment, although the balance between $CD4^+$ and $CD8^+$ subsets was not yet normalized with $CD8^+$ counts still higher than normal and $CD4^+$ counts remaining below normal thresholds. Earlier or stronger therapeutic interventions should reasonably achieve better reversibility.

REFERENCES AND NOTES

1. M. Markowitz *et al.*, *N. Engl. J. Med.* **333**, 1534 (1995); R. Gulick *et al.*, in *Third National Conference on Human Retroviruses and Related Diseases*, Washington, DC, 28 January to 1 February 1996; A. C. Collier *et al.*, *N. Engl. J. Med.* **334**, 1011 (1996); D. Mathez *et al.*, *Antiretroviral Ther.*, in press.
2. W. Wei *et al.*, *Nature* **373**, 117 (1995); D. D. Ho *et al.*, *ibid.*, p. 123.
3. D. E. Mosier *et al.*, *ibid.* **375**, 193 (1995).
4. R. B. Effros *et al.*, *AIDS* **10**, F17 (1996); K. C. Wolthers *et al.*, *Science* **274**, 1543 (1996).
5. M. Roederer *et al.*, *J. Clin. Invest.* **95**, 2061 (1995).
6. J. V. Giorgi, *Immunology of HIV Infection* (Plenum, New York, 1996), p. 181.
7. H. C. Lane *et al.*, *N. Engl. J. Med.* **313**, 79 (1985); J. V. Giorgi *et al.*, *J. Immunol.* **138**, 3725 (1987); M. Clerici *et al.*, *J. Clin. Invest.* **82**, 1908 (1988).
8. B. Autran *et al.*, data not shown.
9. M. Merklenslager *et al.*, *Eur. J. Immunol.* **18**, 1653 (1988).
10. T. F. Tedder *et al.*, *J. Immunol.* **134**, 2989 (1985).
11. S. S. Kansas, *Blood* **88**, 3259 (1996).
12. S. M. Schnittman *et al.*, *Proc. Natl. Acad. Sci. U.S.A.* **87**, 6058 (1990).
13. T. Hara *et al.*, *J. Exp. Med.* **164**, 1988 (1986).
14. M. Levacher *et al.*, *Clin. Exp. Immunol.* **90**, 376 (1992); J. V. Giorgi *et al.*, *J. Acquired Immune Defic. Syndr.* **6**, 904 (1993); M. Bofill *et al.*, *AIDS* **10**, 827 (1996).
15. J. Sprent, *Curr. Opin. Immunol.* **5**, 433 (1993); D. F. Tough *et al.*, *Immunol. Rev.* **150**, 129 (1996).
16. C. Aussel *et al.*, *Cell. Immunol.* **155**, 436 (1994).
17. W. Cavert *et al.*, Science **276**, 960 (1997).
18. C. L. Mackall *et al.*, *N. Engl. J. Med.* **332**, 143 (1995).
19. N. J. Borthwick *et al.*, *AIDS* **8**, 431 (1994).
20. A. D. Kelleher *et al.*, *J. Infect. Dis.* **173**, 321 (1996).
21. B. Rocha and H. von Boehmer, *Science* **251**, 1225 (1991).
22. C. Tanchot and B. Rocha, *Eur. J. Immunol.* **25**, 2127 (1995).
23. D. Mathez *et al.*, *Antimicrob. Agents Chemother.* **37**, 2206 (1993).
24. B. Autran *et al.*, *J. Immunol.* **154**, 1408 (1995).

25. We thank the clinicians participating in the therapeutic trial: A. G. Saimot, I. Gorin, G. Pialoux, and P. De Truchis; V. Calvez for analyzing HIV-1 plasma viral load; J. P. Chauvin from Abbott Laboratories for sponsoring the clinical trial; D. Faudot and M. Hirn from Coulter/Immunotech for kindly providing reagents; and SIDACTION and the Agence Nationale de Recherches sur le SIDA for financial support.

12 February 1997; accepted 7 May 1997

Chemical Coupling Between Atmospheric Ozone and Particulate Matter

Z. Meng, D. Dabdub, J. H. Seinfeld*

A major fraction of ambient particulate matter arises from atmospheric gas-to-particle conversion. Attempts to reduce particulate matter levels require control of the same organic and nitrogen oxide (NO_x) emissions that are precursors to urban and regional ozone formation. Modeling of the gas-aerosol chemical interactions that govern levels of particulate components showed that control of gas-phase organic and NO_x precursors does not lead to proportionate reductions of the gas-phase–derived components of atmospheric particles. The chemical coupling between ozone and particulate matter has implications for strategies to achieve the new ozone and particulate matter standards proposed by the U.S. Environmental Protection Agency.

Ozone has historically been regarded as the principal urban and regional air quality problem in the United States (*1*). Epidemiological evidence that urban mortality rates are correlated with mass concentration of fine particulate matter has now focused intense interest on reducing levels of airborne particles (*2*). In November 1996, the U.S. Environmental Protection Agency (EPA) proposed new ozone (O_3) and particulate matter air quality standards (*3*). Because exposure to lower O_3 concentrations over longer periods of time than the current standard (0.12 parts per million averaged over a 1-hour period) is deemed to be of primary relevance, EPA proposed to lower the O_3 standard to 0.08 ppm averaged over an 8-hour period. EPA also proposed to revise the existing particulate matter (PM) standard to add two new $PM_{2.5}$ (particulate matter of diameter less than or equal to 2.5 μm) standards set at 15 μg m^{-3} for the annual mean, and 50 μg m^{-3} over a 24-hour period. Hundreds of counties in the United States in addition to those already in violation of the current standards are estimated to violate either or both of the new O_3 and PM standards (*4*).

Ozone and PM have traditionally been considered as separate problems. However, O_3 and PM are chemically coupled, and this coupling is of profound importance in understanding processes that control the levels of both. Urban and regional ozone abatement strategies have, for more than a decade, been evaluated with three-dimensional atmospheric models by the EPA and state and local agencies (*1*). We report here the application of a three-dimensional, size- and chemically resolved gas-aerosol model to examine how the chemical coupling that exists between O_3 and PM influences joint control of the two classes of pollutants.

The common components of atmospheric particles, such as sulfate (SO_4^{2-}), nitrate (NO_3^-), ammonium (NH_4^+), organic compounds, crustal material, and water, reach the particulate phase by several different processes (Fig. 1). Aside from the direct emission of particles into the atmosphere, gas-to-particle conversion processes play an essential role in determining the mass of airborne PM. Such processes depend intimately on the organic

Z. Meng, Department of Environmental Engineering Science, California Institute of Technology, Pasadena, CA 91125, USA.
D. Dabdub, Department of Mechanical and Aerospace Engineering, University of California, Irvine, CA 92717–3975, USA.
J. H. Seinfeld, Department of Chemical Engineering and Division of Engineering and Applied Science, California Institute of Technology, Pasadena, CA 91125, USA.

*To whom correspondence should be addressed. E-mail: john_seinfeld@starbase1.caltech.edu